








Cite this: DOI: 10.1039/c9cy02016k

Piperazine-promoted gold-catalyzed hydrogenation: the influence of capping ligands†

Jhonatan L. Florio, ^a Eduardo C. M. Barbosa, ^a Danielle K. Kikuchi,^a
Pedro H. C. Camargo, ^a Matthias Rudolph,^b
A. Stephen K. Hashmi ^b and Liane M. Rossi ^{*a}

Gold nanoparticles (NPs) combined with Lewis bases, such as piperazine, were found to perform selective hydrogenation reactions *via* the heterolytic cleavage of H₂. Since gold nanoparticles can be prepared by many different methodologies and using different capping ligands, in this study, we investigated the influence of capping ligands adsorbed on gold surfaces on the formation of the gold–ligand interface. Citrate (Cit), poly(vinyl alcohol) (PVA), polyvinylpyrrolidone (PVP), and oleylamine (Oley)-stabilized Au NPs were not activated by piperazine for the hydrogenation of alkynes, but the catalytic activity was greatly enhanced after removing the capping ligands from the gold surface by calcination at 400 °C and the subsequent adsorption of piperazine. Therefore, the capping ligand can limit the catalytic activity if not carefully removed, demonstrating the need of a cleaner surface for a ligand–metal cooperative effect in the activation of H₂ for selective semihydrogenation of various alkynes under mild reaction conditions.

Received 7th October 2019,
Accepted 28th November 2019

DOI: 10.1039/c9cy02016k

rsc.li/catalysis

Introduction

Colloidal metal nanoparticles (NPs) are often prepared by colloidal synthesis methods and stabilized in solution by the interaction of specific capping ligands with the surface, which ensures that the nanoparticles do not coalesce.^{1,2} This type of methodology has received attention for the preparation of supported catalysts, allowing the preparation of metal catalysts with high control over particle size, shape, and surface composition.^{3–5} The major concern of using colloidal synthetic methods is the influence of capping ligands adsorbed on the metallic surface both on the immobilization efficiency and on the catalyst performance, due to their binding affinity to the metallic surface.^{6–8} Overall, the presence of capping ligands can also decrease the accessibility of substrates to the metal surface or metal–support interface,^{9–11} causing low catalytic activity, since reactants cannot bind to surface atoms and undergo chemical transformations into the desired products.^{12–15}

Based on the assumption that the catalytic activity is diminished if the surface of metal nanoparticles is partly covered

by capping ligands, until very recently, ligands were often removed either by extraction or pyrolysis before catalytic applications.^{16–18} However, it has been discussed that the capping ligands could be a dynamic component of the active catalyst which improves selectivity and activity.^{19–26} We recently demonstrated an enhancement in the catalytic activity of gold nanocatalysts when using amine ligands as an additive in the reaction medium. The combination of the added amine ligand (Lewis base) and the gold surface (Lewis acid) triggered the heterolytic activation of molecular hydrogen *via* a frustrated Lewis pair-like mechanism, allowing an unexpectedly high activity in an alkyne semi-hydrogenation reaction.²⁷ This behavior has been demonstrated with gold catalysts prepared by an impregnation–reduction method, therefore free of capping ligands; however, since capping ligands are generally present when the synthesized colloidal nanoparticles are used in catalysis, a systematic study analyzing the effect of capping ligands on the formation of the piperazine–gold interface is missing.²⁸

Herein, we investigate how capping ligands adsorbed on the surface of Au NPs can hinder the formation of the piperazine–gold interface needed to activate H₂ in hydrogenation reactions. Our studies reveal that the presence of capping ligands blocks the adsorption of the amine onto the gold surface, thereby leading to low catalytic activity. When the capping ligands were removed from the catalyst surface and the piperazine ligand was added, enhanced catalytic activity was observed.

^a Departamento de Química Fundamental, Instituto de Química, Universidade de São Paulo, Av. Prof. Lineu Prestes, 748, 05508-000, São Paulo, SP, Brazil

^b Organisch-Chemisches Institut, Ruprecht-Karls-Universität Heidelberg University, Im Neuenheimer Feld 270, 69120 Heidelberg, Germany. E-mail: lrossi@iq.usp.br

† Electronic supplementary information (ESI) available. See DOI: 10.1039/c9cy02016k

Experimental section

Preparation of Au_{PVA}/C

The gold catalyst stabilized with PVA (average molecular weight MW = 9000–10 000 g mol⁻¹, 80% hydrolyzed) was prepared as previously described in the literature^{16,29} as follows: to an aqueous HAuCl₄ solution (5.08 × 10⁻⁴ mol L⁻¹), the required amount of a PVA solution (1 wt%) was added (PVA/(Au) (w/w) = 1.2), and a freshly prepared solution of NaBH₄ (0.1 mol L⁻¹, NaBH₄/(Au)(mol/mol) = 5) was then added to form a dark-brown sol. After 30 min of sol generation, 1 g of the carbon support (Vulcan XC 72R) was added to the colloid, and the mixture was vigorously stirred overnight to immobilize the Au NPs in the support. The slurry was filtered, and the catalyst was washed three times with acetone and dried under vacuum. The final metal loading was 0.7 wt% as determined by FAAS.

Preparation of Au_{PVP}/C

The gold nanoparticles stabilized with PVP were prepared according to a procedure reported elsewhere.^{30,31} In a typical synthesis of 1 g of Au_{PVP}/C, an aqueous solution of HAuCl₄·3H₂O (0.8 mL, 25 mg HAuCl₄·3H₂O per mL Sigma Aldrich, ≥49.0%) was added to 400 mL of deionized water under vigorous stirring conditions, followed by the addition of a 1 wt% aqueous solution of PVP (Sigma Aldrich, average molecular weight MW = 10 000 g mol⁻¹). Next, a 0.1 M freshly prepared solution of NaBH₄ was added (mol NaBH₄ per mol Au = 5) to form a red sol. After 30 min of sol generation, the colloid was immobilized by adding 1 g of carbon support (Vulcan XC 72R). The mixture was stirred overnight. After, the slurry was filtered, and the catalyst was washed three times with acetone and dried under vacuum. The metal loading was 0.5 wt% as determined by FAAS.

Preparation of Au_{Oleylamine}/C

In a typical synthesis as described elsewhere,³² 10 mL of tetralin, 10 mL of oleylamine and 278.4 mg of HAuCl₄ were added to a three-neck round-bottom flask and the mixture was magnetically stirred under a N₂ flow for 10 min, at 35 °C. After, a reducing solution containing 0.5 mmol of TBAB, tetralin (1 mL), and oleylamine (1 mL) was prepared by sonication and injected all at once into the precursor solution. The reduction was instantaneously initiated, and the solution changed to a deep purple color. The mixture was allowed to react at 35 °C for 1 h before 1 g of carbon support was added and vigorously stirred overnight. The slurry was filtered, washed three times with acetone and dried under vacuum. The metal content was 0.5 wt% as determined by FAAS.

Preparation of Au_{Citrate}/C

To prepare the gold catalyst stabilized with citrate, we adopted a previously described method in the literature.³³ A typical procedure is as follows: to a three-neck round-bottom flask was added a freshly prepared aqueous solution of

sodium citrate (150 mL, 2.2 mM), tannic acid (0.1 mL, 2.5 mM) and K₂CO₃ (1 mL, 150 mM), and the resulting solution was heated in a heating mantle to 70 °C. Once the temperature reached 70 °C, 1 mL of HAuCl₄ (25 mM) was injected. The solution was kept at 70 °C for an additional 5 min to ensure complete reaction of the gold precursor. After, 1 g of the carbon support was added, and the mixture was stirred overnight to immobilize the Au NPs. The catalyst was collected by centrifugation, washed three times with acetone and dried under vacuum. The metal content was 0.4 wt% as determined by FAAS.

Thermal treatment to remove the ligand

Typically, to remove the ligand from the catalyst surface a certain amount of the as-prepared catalyst was placed in a crucible and the solid was thermally treated in an oven at a rate of 10 °C per minute and held at 400 °C for 2 h under a N₂ atmosphere. Instead of being calcined, a set of catalysts were refluxed with water as previously described in the literature¹⁶ to remove the excess ligand, and then dried under vacuum.

Catalytic investigations

Catalytic hydrogenation reactions

In a modified Fischer–Porter 100 mL glass reactor, the substrate (1 mmol), piperazine (1 mmol) and gold catalyst (0.5 mol%) were mixed with 2 mL of ethanol. The reactor was closed and purged five times with H₂, leaving the vessel at 6 bar of H₂. All the reactions were performed at 80 °C; the temperature was maintained with an oil bath on a stirring hot plate. After the completion of the reaction, the catalyst was removed by centrifugation and the products were analyzed by GC with an internal standard to determine the conversion of the substrate and the selectivity for the product.

Recycling experiment

In a typical recycling experiment, the substrate (1 mmol), piperazine (100 eq.) and gold catalyst (1 mol%) were added to a Fischer–Porter 100 mL glass reactor equipped with a magnetic stirring bar, the reactor was then closed, purged five times with H₂, leaving the vessel at 6 bar of H₂, and the resulting reaction mixture was heated at 80 °C for 24 h. After the reaction was complete, the reactor was cooled to room temperature and the hydrogen was released. An internal standard (biphenyl) was added to the solution to determine the conversion and selectivity by GC analysis of the mixture. The catalyst separated by centrifugation was washed with ethanol three times, then dried under vacuum, and reused for the next reaction.

Product analysis of catalytic experiments

All the products were determined by GC analyses carried out with a Shimadzu GC-2010 equipped with an RTx-5 column (30 m × 0.25 mm × 0.25 mm) and a FID (all GC yields are

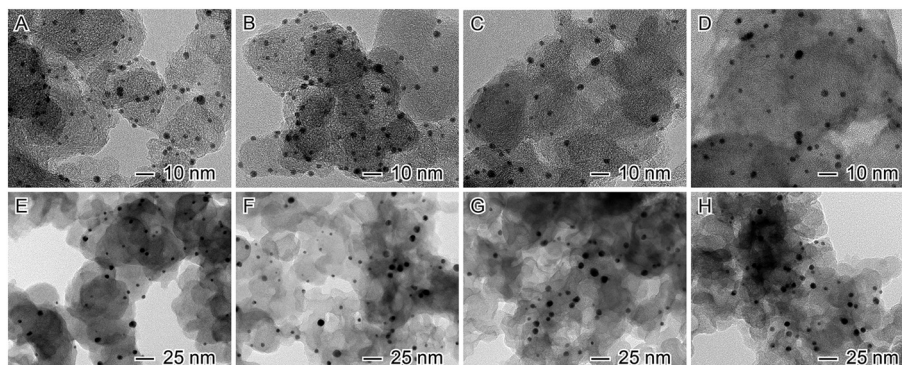


Fig. 1 TEM images of nanoparticles before and after thermal treatment at 400 °C (A and E) Au_{PVA}/C, (B and F) Au_{PVP}/C, (C and G) Au_{Oley}/C, and (D and H) Au_{Citr}/C.

average values from at least 2 runs). Method: Ti = 40 °C, Tf = 200 °C, 17 min. Internal standard: biphenyl. The conversion and selectivity were determined from the total amount of the detected products and reactant.

High pressure NMR studies

All the reactions were analyzed using a Bruker Avance DRX 300 MHz at 80 °C. The Au_{PVA} nanoparticles were extensively washed to remove the excess stabilizer before analysis. The gold colloid, piperazine and deuterated solvent (D₂O) were added to a high pressure NMR tube, which was pressurized with 10 bar of H₂ and heated to the desired temperature. The reactions were monitored using ¹H NMR spectroscopy.

Results and discussion

Colloidal Au NPs with various capping ligands but with similar sizes were prepared by different methodologies to

evaluate the effect of each capping ligand on the catalytic activity while avoiding possible size-dependent effects. The colloidal Au NPs with different capping ligands were immobilized on carbon and the TEM analyses of the supported Au/C catalysts confirmed the uniform dispersion over the support and the control over the NP size (Fig. 1A–D). The corresponding particle size distributions (Fig. S2†) indicate that the mean particle size of each sample is ~3 nm. To remove the ligand from the catalyst surface and compare the adsorption of the amine ligand on a clean surface with that on a surface occupied by capping ligands, we conducted a thermal treatment in a portion of the as-prepared catalyst. An obvious increase in size was observed for all the catalysts (Fig. 1E–H), and the mean diameter after thermal treatment was ~8 nm (Fig. S2†). Different UV-vis spectrum profiles for the catalysts were noticed (Fig. S1†), suggesting that the electronic structure of the Au NPs can be disturbed by the surrounding organic ligands or it might be related to the

Table 1 Catalytic activity of Au catalysts in the hydrogenation of phenylacetylene **1a**^a

Entry	Catalyst	Calcined at 400 °C	Amine	Conversion (%)	Selectivity to 2a (%)
1	Au _{PVA} /C	No	No	6	>99
2	Au _{PVA} /C	No	Yes	3	>99
3	Au _{PVA} /C	Yes	No	8	>99
4	Au _{PVA} /C	Yes	Yes	>99	>99
5	Au _{Citr} /C	No	No	5	>99
6	Au _{Citr} /C	No	Yes	3	>99
7	Au _{Citr} /C	Yes	No	2	>99
8	Au _{Citr} /C	Yes	Yes	70	94
9	Au _{Oley} /C	No	No	2	>99
10	Au _{Oley} /C	No	Yes	3	>99
11	Au _{Oley} /C	Yes	No	4	>99
12	Au _{Oley} /C	Yes	Yes	68	85
13	Au _{PVP} /C	No	No	3	>99
14	Au _{PVP} /C	No	Yes	6	>99
15	Au _{PVP} /C	Yes	No	8	>99
16	Au _{PVP} /C	Yes	Yes	82	>99

^a Reaction conditions: 1 mmol of alkyne, 0.5 mol% Au, 1 mmol of piperazine, 2 mL of EtOH, 80 °C, 6 bar of H₂, 24 h. Conversion and selectivity were determined by GC using the internal standard technique.

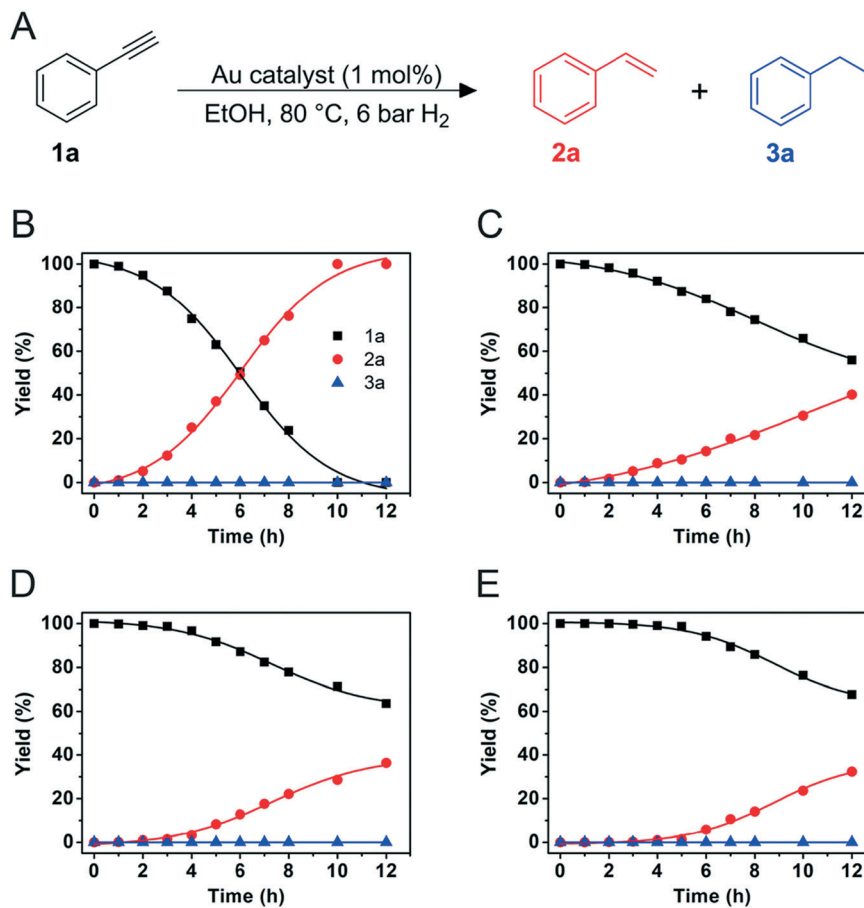


Fig. 2 A) Time course studies comparing the reaction profile of the calcined catalysts at 400 °C with addition of piperazine in the hydrogenation of phenylacetylene; B) Au_{PVA}/C ; C) Au_{PVP}/C ; D) Au_{Citric}/C ; E) Au_{Oleyl}/C ; reaction conditions: 4 mmol of alkyne, 0.5 mol% Au, 4 mmol of piperazine, 8 mL of EtOH, 80 °C, 6 bar of H_2 .

differences in size distribution; both factors may cause a shift in the surface plasmon resonance dipole mode of the Au NPs.^{34–36} Characteristic absorption bands related to the corresponding protective agents were observed in the FTIR spectra of the as-prepared samples (Fig. S3a–d†). In the thermally treated catalyst, no typical band of the capping ligand was observed, confirming the removal from the catalyst surface (Fig. S4†).

It is anticipated that the capping ligands on the surface of the Au NPs might affect the adsorption of piperazine, possibly blocking the formation of the piperazine–gold interface.^{37,38} Here, we examined the hydrogenation of phenylacetylene as a model transformation under conditions optimized elsewhere (6 bar of H_2 , piperazine as a ligand and 80 °C)²⁷ using the as-prepared supported Au NP catalysts (mean diameter size ~3 nm) with different capping ligands (PVA, citrate, oleylamine and PVP) and their thermally treated counterparts (mean diameter size ~8 nm). All the catalysts (as-prepared and thermally treated) reached very low conversions in the absence of piperazine (Table 1, entries 1, 3, 5, 7, 9, 11, 13 and 15). Typically, the as-prepared Au catalysts, which contain capping ligands and smaller NPs, were less active than the thermally treated Au catalysts

(Table 1, entries 4, 8, 12 and 16). This trend suggests that the capping ligands restrict the free access of the reactants to the catalytically active sites on the Au NP surface and/or prevent the adsorption of piperazine, which is crucial to lowering the energy barrier for H_2 dissociation.²⁷ Once these capping

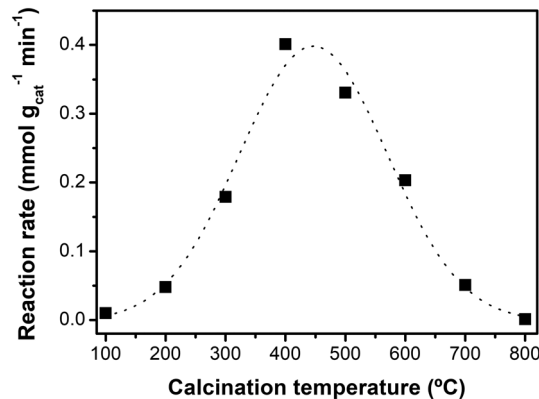


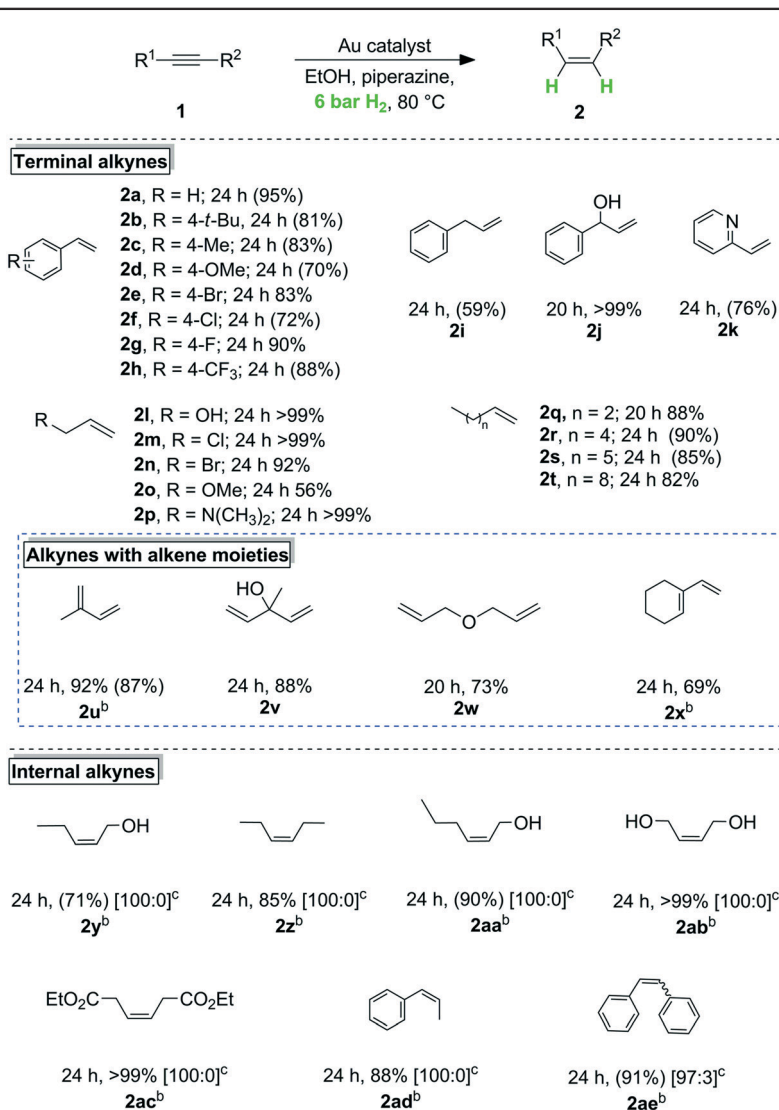
Fig. 3 Reaction rate performance of the Au_{PVA}/C catalyst thermally treated at different temperatures in the hydrogenation of phenylacetylene.

ligands were removed from the Au NP surface, the addition of piperazine promoted the favorable activation of H₂, leading to a high conversion of **1a** and a high selectivity to the alkene product **2a** (Table 1, entries 4, 8, 12 and 16). The behavior reproduces that of the Au–piperazine ligand system reported before,²⁷ suggesting that piperazine plays a dual role in the activation of Au NPs as an activity and selectivity enhancer.

Kinetic studies were carried out with the four most active catalytic systems (Fig. 2). Notably, the thermally treated Au_{PVA}/C in the presence of piperazine is the most active catalytic system, reaching full conversion and high selectivity to **2a**. The reaction rates for the thermally treated Au_{PVP}/C, Au_{Citr}/C, and Au_{Oley}/C are significantly lower. The initial lower activity (activation time) might be due to carbonaceous

residues formed during the thermal treatment. However, considering that all the catalysts are supported on carbon, it is difficult to quantitatively determine any change in the carbon content before and after calcination (Table S2†). No significant size change was noticed among the different capping ligands (~8 nm) to justify the difference in activity (Fig. S2†). Instead of calcination, the as-prepared Au_{PVA} and Au_{Citr} catalysts were subjected to a milder method to remove the capping ligands, as reported in the literature.^{16,17} Both catalysts were washed with water under reflux at 90 °C to remove the excess capping ligand and then tested in the hydrogenation reaction with and without piperazine (Table S3†). The washed catalysts became slightly more active, but the addition of piperazine promoted an activity enhancement as seen in the calcined samples, suggesting that this method

Table 2 Semihydrogenation of various alkynes to alkenes^a



^a Reaction conditions: 1 mmol of alkyne, 0.5 mol% Au (Au_{PVA}/C calcined at 400 °C), 1 mmol of piperazine, 2 mL of EtOH, 80 °C, 6 bar of H₂. Conversion and selectivity were determined by GC using the internal standard technique. In all cases, the selectivity was >99%. Isolated yields in parenthesis. ^b 1 mol% Au. ^c Determined by ¹H NMR.

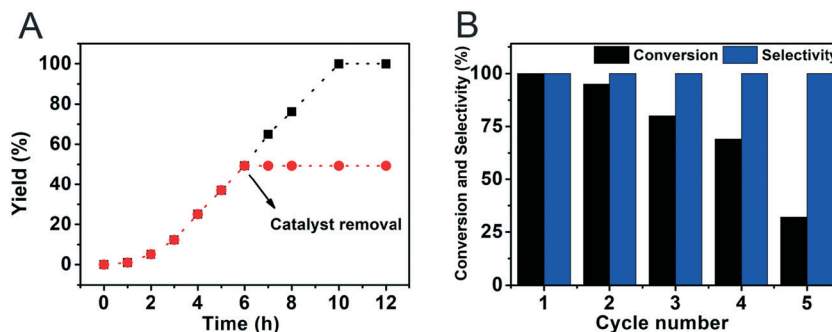


Fig. 4 A) Hot filtration test and B) recycling experiments for hydrogenation of phenylacetylene.

is also effective in removing the capping ligands for improving the accessibility of piperazine to the Au NPs surface.

At this point, we studied the influence of the calcination temperature on the reaction rate, using the Au_{PVA}/C catalyst as a model. As shown in Fig. 3, the calcination temperature and catalytic activity exhibit a volcano-type relationship. The reaction rate increases with the calcination temperature (ranging from 200 to 400 °C), reaching its maximum, and abruptly decreases at higher temperatures. The drop in the reaction rate at higher temperatures is due to nanoparticle sintering as verified by TEM analysis of the catalysts (Fig. S5†).¹⁶ The low catalytic activity at lower calcination temperatures may happen due to the presence of capping ligands blocking the adsorption of the amine ligand.

The catalytic potential of Au_{PVA}/C thermally treated at 400 °C, which exhibited the best performance, was investigated using various alkynes. Ethynylbenzenes bearing electron-donating and electron-withdrawing groups were selectively hydrogenated to the corresponding terminal alkenes with excellent selectivity, and reducible functional groups, such as halogen and hydroxyl moieties, were tolerated (Table 2, entries 2a–2t). Various aliphatic terminal alkynes were also efficiently converted into their corresponding terminal alkenes without isomerization into internal alkenes (Table 2, entries 2u–2x). Importantly, alkynes with an alkene moiety were smoothly hydrogenated, whereas alkene moieties in the parent and product molecules were completely intact (Table 2, entries 2q–2t). Moreover, a series of internal alkynes were smoothly hydrogenated to the Z-alkenes in excellent diastereoselectivity (Table 2, entries 2y–2ae).

Considering that heterogeneous catalysts, especially in the presence of ligands, may act as a reservoir for highly active leached species, a hot filtration test was carried out in order to detect whether soluble active Au species were responsible for the observed catalytic activity. After the first reaction under standard conditions, the catalysts were filtered off when the second reaction reached average 50% conversion and no further conversion was observed when the reaction was continued using the hot filtrate solution only (Fig. 4A). This experiment excludes the presence of active solubilized species. The recovered solid catalyst was reusable, but a significant decrease in the catalytic activity was noticed after the third cycle, though the selectivity towards the alkene was

maintained through all the cycles (Fig. 4B). After each reaction, the catalyst was separated by filtration and the filtrate was analyzed by inductively coupled plasma atomic emission spectrometry (ICP AES) analysis, which revealed that no leaching of Au species in the reaction mixture occurred (detection limit: 0.1 ppm) (Table S1†). TEM analysis of the recycled catalyst (Fig. S6†) revealed that the decrease in the catalytic activity can be due to a significant increase in the mean diameter size of the Au NPs to ~20 nm. Therefore, as previously described, the capping ligand might play an important role in preventing the agglomeration of the nanoparticles and increasing the lifetime of the catalyst. However, once the capping ligand is completely removed, a drop in the activity is observed over the recycling process.⁶

Altogether, the above catalytic results imply that, as previously described, piperazine once adsorbed on the Au surface facilitates the heterolytic H₂ activation at the Au NPs.^{24,38–42} However, the presence of capping ligands on the surface of Au NPs avoids the adsorption of the amine ligand (Fig. 5), providing an unfavorable situation for hydrogen activation. Effective removal of the capping ligand by thermal treatment exposes the nanoparticles' surfaces and thus enhances the catalytic activity, as a result of the successful formation of the piperazine–gold interface, which promotes the molecular hydrogen splitting, the rate-determining step of the reaction.

To gain insight into the nature of the catalytic active species, NMR investigations were carried out using the Au_{PVA}

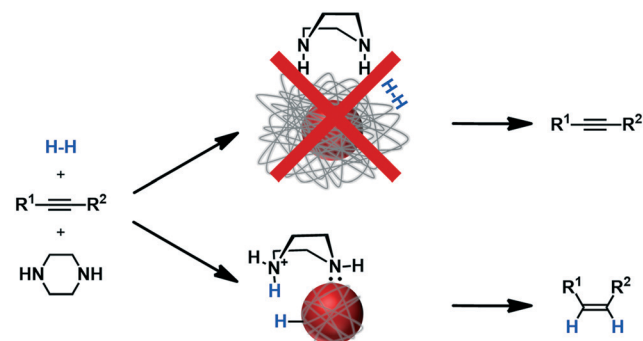


Fig. 5 Scheme showing the differences in the activity of Au NPs with and without a capping ligand.

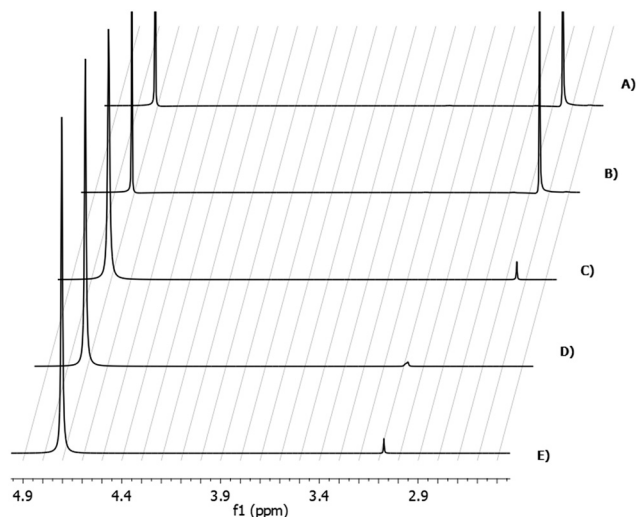


Fig. 6 Overlay of the ^1H NMR spectra of (A) piperazine, (B) piperazine/ H_2 (10 bar), (C) piperazine/Au colloid, (D) piperazine/Au colloid/ H_2 (10 bar) and (E) piperazine/Au colloid/ H^+ in D_2O .

NPs and piperazine. The Au colloid was thoroughly washed to remove the excess capping ligand before analysis. Fig. 6 shows the proton NMR spectra of piperazine solutions in D_2O at 80°C with and without the Au colloid. Either the free ligand (Fig. 6A) or the free ligand under H_2 pressure (Fig. 6B) exhibits similar signals around 2.7 (4H, N-H) and 4.8 ppm (8H, CH_2). In the presence of the Au colloid, the signal remains at 2.7 ppm, but decreases in intensity, most probably due to H/D-exchange (Fig. 6C). As observed in Fig. 6D, when the solution of piperazine with Au colloid was pressurized with H_2 (10 bar), a new signal appeared at 3.1 ppm. A signal with a similar chemical shift was also observed when a piperazine solution was acidified (Fig. 6E), which is in agreement with the literature value.⁴³ Therefore, the signal at 3.1 ppm may be assigned to protonated piperazine species, which are formed in acidic media and through dissociation of H_2 . Therefore, these results suggest that a ligand to metal cooperative effect causes the H_2 dissociation, *via* a heterolytic mechanism, leading to the protonation of the ligand, which is in sharp agreement with the mechanism suggested in previously reported studies.^{27,44–46}

Conclusions

In conclusion, we have studied the limitations of using Au NPs with different capping ligands for the preparation of piperazine-gold interfaces necessary to boost gold activity towards hydrogenation reactions. The presence of capping agents blocks the adsorption of the amine ligand leading to low catalytic activity. The removal of the stabilizing agents by thermal treatment, which allows the successful adsorption of the amine ligand, leads to an increase in the catalytic activity. Moreover, the catalytic system enables the highly selective semi-hydrogenation of various alkynes under mild reaction conditions, with excellent selectivity for alkenes. This work

represents a clear demonstration of the ligand-metal cooperative effect in the activation of H_2 , where the nature of the capping ligand plays a crucial role and can limit the catalytic activity if not carefully removed.

Conflicts of interest

There are no conflicts to declare.

Acknowledgements

The authors are grateful to INCT-Catálise and the Brazilian government agencies FAPESP (2016/16738-7, 2015/21366-9, and 2015/26308-7), CNPq, the Serrapilheira Institute (grant number Serra-1709-16900), and CAPES for financial support. E. C. M. B. thanks FAPESP for the fellowship (2015/11452-5) and J. L. F. also thanks CAPES-DAAD-CNPQ for his scholarship (Grant 88887.161404/2017-00).

Notes and references

- N. T. K. Thanh, N. Maclean and S. Mahiddine, *Chem. Rev.*, 2014, **114**, 7610–7630.
- Y. Xia, Y. Xiong, B. Lim and S. E. Skrabalak, *Angew. Chem., Int. Ed.*, 2009, **48**, 60–103.
- P. Sonström and M. Bäumer, *Phys. Chem. Chem. Phys.*, 2011, **13**, 19270–19284.
- C.-J. Jia and F. Schüth, *Phys. Chem. Chem. Phys.*, 2011, **13**, 2457–2487.
- L. S. Ott and R. G. Finke, *Coord. Chem. Rev.*, 2007, **251**, 1075–1100.
- A. Villa, D. Wang, G. M. Veith, F. Vindigni and L. Prati, *Catal. Sci. Technol.*, 2013, **3**, 3036.
- R. Y. Zhong, K. Q. Sun, Y. C. Hong and B. Q. Xu, *ACS Catal.*, 2014, **4**, 3982–3993.
- P. Munnik, P. E. de Jongh and K. P. de Jong, *Chem. Rev.*, 2015, **115**, 6687–6718.
- C. Kartusch and J. A. van Bokhoven, *Gold Bull.*, 2009, **42**, 343–348.
- T. Whittaker, K. B. S. Kumar, C. Peterson, M. N. Pollock, L. C. Grabow and B. D. Chandler, *J. Am. Chem. Soc.*, 2018, **140**, 16469–16487.
- J. E. Bruno, K. B. Sravan Kumar, N. S. Dwarica, A. Hüther, Z. Chen, C. S. Guzman, E. R. Hand, W. C. Moore, R. M. Rioux, L. C. Grabow and B. D. Chandler, *ChemCatChem*, 2019, **11**, 1650–1664.
- A. S. K. Hashmi and G. J. Hutchings, *Angew. Chem., Int. Ed.*, 2006, **45**, 7896–7936.
- L. M. Rossi, J. L. Fiorio, M. A. S. Garcia and C. P. Ferraz, *Dalton Trans.*, 2018, **47**, 5889–5915.
- S. Campisi, M. Schiavoni, C. Chan-Thaw and A. Villa, *Catalysts*, 2016, **6**, 185.
- Q. Wang, M. Ming, S. Niu, Y. Zhang, G. Fan and J.-S. Hu, *Adv. Energy Mater.*, 2018, **1801698**, 1801698.
- J. A. Lopez-Sanchez, N. Dimitratos, C. Hammond, G. L. Brett, L. Kesavan, S. White, P. Miedziak, R. Tiruvalam, R. L.

- Jenkins, A. F. Carley, D. Knight, C. J. Kiely and G. J. Hutchings, *Nat. Chem.*, 2011, **3**, 551–556.
- 17 Z. Niu and Y. Li, *Chem. Mater.*, 2014, **26**, 72–83.
- 18 G. Collins, F. Davitt, C. O'Dwyer and J. D. Holmes, *ACS Appl. Nano Mater.*, 2018, **1**, 7129–7138.
- 19 J. Zhang, L. D. Ellis, B. Wang, M. J. Dzara, C. Sievers, S. Pylypenko, E. Nikolla and J. W. Medlin, *Nat. Catal.*, 2018, **1**, 148–155.
- 20 M. Makosch, W.-I. Lin, V. Bumbálek, J. Sá, J. W. Medlin, K. Hungerbühler and J. A. van Bokhoven, *ACS Catal.*, 2012, **2**, 2079–2081.
- 21 G. Chen, C. Xu, X. Huang, J. Ye, L. Gu, G. Li, Z. Tang, B. Wu, H. Yang, Z. Zhao, Z. Zhou, G. Fu and N. Zheng, *Nat. Mater.*, 2016, **15**, 564.
- 22 P. Hao, S. Pylypenko, D. K. Schwartz and J. W. Medlin, *J. Catal.*, 2016, **344**, 722–728.
- 23 S. G. Kwon, G. Krylova, A. Sumer, M. M. Schwartz, E. E. Bunel, C. L. Marshall, S. Chattopadhyay, B. Lee, J. Jellinek and E. V. Shevchenko, *Nano Lett.*, 2012, **12**, 5382–5388.
- 24 B. Wu, H. Huang, J. Yang, N. Zheng and G. Fu, *Angew. Chem., Int. Ed.*, 2012, **51**, 3440–3443.
- 25 N. Kaeffer, H. J. Liu, H. K. Lo, A. Fedorov and C. Copéret, *Chem. Sci.*, 2018, **9**, 5366–5371.
- 26 J. L. Fiorio, R. V. Gonçalves, E. Teixeira-Neto, M. A. Ortuño, N. López and L. M. Rossi, *ACS Catal.*, 2018, **8**, 3516–3524.
- 27 J. L. Fiorio, N. López and L. M. Rossi, *ACS Catal.*, 2017, **7**, 2973–2980.
- 28 S. Arndt, M. Rudolph and A. S. K. Hashmi, *Gold Bull.*, 2017, **50**, 267–282.
- 29 F. Porta, L. Prati, M. Rossi, S. Coluccia and G. Martra, *Catal. Today*, 2000, **61**, 165–172.
- 30 N. Agarwal, S. J. Freakley, R. U. McVicker, S. M. Althahban, N. Dimitratos, Q. He, D. J. Morgan, R. L. Jenkins, D. J. Willock, S. H. Taylor, C. J. Kiely and G. J. Hutchings, *Science*, 2017, **358**, 223–227.
- 31 L. Abis, S. J. Freakley, G. Dodekatos, D. J. Morgan, M. Sankar, N. Dimitratos, Q. He, C. J. Kiely and G. J. Hutchings, *ChemCatChem*, 2017, **9**, 2914–2918.
- 32 S. Peng, Y. Lee, C. Wang, H. Yin, S. Dai and S. Sun, *Nano Res.*, 2008, **1**, 229–234.
- 33 J. Piella, N. G. Bastús and V. Puntes, *Chem. Mater.*, 2016, **28**, 1066–1075.
- 34 X.-K. Wan, J.-Q. Wang, Z.-A. Nan and Q.-M. Wang, *Sci. Adv.*, 2017, **3**, e1701823.
- 35 K. L. Kelly, E. Coronado, L. L. Zhao and G. C. Schatz, *J. Phys. Chem. B*, 2003, **107**, 668–677.
- 36 R.-Y. Zhong, X.-H. Yan, Z.-K. Gao, R.-J. Zhang and B.-Q. Xu, *Catal. Sci. Technol.*, 2013, **3**, 3013.
- 37 L. Wang, G. Kehr, C. G. Daniliuc, M. Brinkkötter, T. Wiegand, A.-L. Wübker, H. Eckert, L. Liu, J. G. Brandenburg, S. Grimme and G. Erker, *Chem. Sci.*, 2018, **9**, 4859–4865.
- 38 Y. Ma, S. Zhang, C.-R. Chang, Z.-Q. Huang, J. C. Ho and Y. Qu, *Chem. Soc. Rev.*, 2018, **47**, 5541–5553.
- 39 D. Ren, L. He, L. Yu, R.-S. Ding, Y.-M. Liu, Y. Cao, H.-Y. He and K.-N. Fan, *J. Am. Chem. Soc.*, 2012, **134**, 17592–17598.
- 40 K. K. Ghuman, L. B. Hoch, T. E. Wood, C. Mims, C. V. Singh and G. A. Ozin, *ACS Catal.*, 2016, **6**, 5764–5770.
- 41 D. W. Stephan, *Science*, 2016, **354**, aaf7229.
- 42 G. Lu, P. Zhang, D. Sun, L. Wang, K. Zhou, Z.-X. Wang and G.-C. Guo, *Chem. Sci.*, 2014, **5**, 1082–1090.
- 43 P. I. Nagy, A. Maheshwari, Y.-W. Kim and W. S. Messer, *J. Phys. Chem. B*, 2010, **114**, 349–360.
- 44 N. Kaeffer, K. Larmier, A. Fedorov and C. Copéret, *J. Catal.*, 2018, **364**, 437–445.
- 45 W. Liu, Y. Chen, H. Qi, L. Zhang, W. Yan, X. Liu, X. Yang, S. Miao, W. Wang, C. Liu, A. Wang, J. Li and T. Zhang, *Angew. Chem., Int. Ed.*, 2018, **57**, 7071–7075.
- 46 R. Lin, D. Albani, E. Fako, S. K. Kaiser, O. V. Safonova, N. López and J. Pérez-Ramírez, *Angew. Chem., Int. Ed.*, 2019, **58**, 504–509.